Title: Topology-Dependent Interference of Synthetic Gene Circuits by Growth Feedback

Rong Zhang[1,#], Jiao Li[1,2,#], Juan Melendez-Alvarez[1], Xingwen Chen[1], Patrick Sochor[1], Qi Zhang[1], Hanah Goetz[1], Tian Ding[2], Xiao Wang[1,*], and Xiao-Jun Tian[1,*]

[1]School of Biological and Health Systems Engineering, Arizona State University, Tempe, AZ 85281, United States of America,

[2]Department of Food Science and Nutrition, Zhejiang University, Hangzhou, Zhejiang, China

#These authors contributed equally to this work

*To whom correspondence should be addressed:

(Lead Contact) Xiao-Jun Tian, Ph.D., School of Biological and Health Systems Engineering, Arizona State University, Tempe, AZ, 85287, xiaojun.tian@asu.edu.

Xiao Wang, Ph.D., School of Biological and Health Systems Engineering, Arizona State University, Tempe, AZ, 85287, xiao.wang@asu.edu.

Abstract

Growth-mediated feedback between synthetic gene circuits and host organisms leads to various emerged behaviors, including innate growth bistability and increased ultrasensitivity. However, the adverse impact of growth feedback on gene circuits remains unexplored. Here, we found that the effects of growth feedback on the functional perturbations of gene circuits depend on the network topology. Specifically, the memory of a self-activation circuit is lost due to the fast growth of host cells. Decoupling of growth feedback reveals its hysteresis property in a broad range. Interestingly, the toggle switch circuit is more refractory to the growth feedback. The underlying principle is demonstrated by modeling the interplay between microbial growth and the gene circuit. Our results reveal a topology-dependent mechanism underlying the functional perturbation of gene circuits by growth-mediated feedback.

INTRODUCTION

Circuit-host interactions add an additional hidden layer to synthetic gene circuits and perturb the behaviors of these circuits [1-3]. There are many sources of circuit-host interactions, including metabolic burden [4, 5], cell growth [6-9], and resource relocation/competition [7, 10-12]. These interactions are often neglected when designing gene circuits by assuming that the gene circuits are orthogonal to the host background [13-16]. However, in many cases, the impacts of interactions between the gene circuit and the host organism are significant [17-19]. Thus, understanding the mechanisms of how circuit-host mutual interactions are established, particularly how their interactions affect gene circuit functions, will help us to better formulate control strategies for designing and engineering robust gene circuits that ensure more accurate applications.

Furthermore, feedback loops are created by mutual circuit-host interactions. For example, growth feedback is formed, given that the expression of the synthetic gene circuits inevitably causes metabolic burden to the host cells and thus affects the cell growth, and it in turn changes the gene expression of circuits [20, 21]. Growth-mediated feedback can endow the synthetic gene circuits with various emerged properties. For example, a non-cooperative positive autoregulatory system, when coupled with growth-mediated feedback, gains significant cooperativity and thus resulted in bistability [22, 23]. Innate growth bistability arises in drug-resistant bacteria when an antibiotic resistance gene expression is coupled to cell growth [24]. Toxin cooperativity can also be induced in the multiple toxin-antitoxin systems with several growth-mediated feedbacks [25]. However, the desired function of gene circuits could be attenuated or disabled by the growth-mediated feedback and thus may not be evaluated accurately.

Here we are interested in whether the network topology affects the extent to which the growth feedback influences the gene circuit behaviors. We compared memory gene circuits with different topologies to test whether the circuit-host interaction can negatively affect circuits. There are

several works on the synthetic bistable switch circuits, including the toggle switch, self-activation switch, push-on-push-off switch, and quadrastable switch [26-29]. To test the hysteresis properties of these circuits, a dilution protocol is often used to make sure the cells are in the exponential growth phase. For example, in the seminal work of the toggle switch, all the samples are washed and diluted into fresh medium every 6-10 hours [26]. The underlying reason is that the cell growth can be maintained in a relatively constant rate and the activity of the promoters in the gene circuits are relatively strong. While this dilution protocol works successfully to demonstrate the hysteresis properties of these circuits, an issue naturally arises concerning whether constant cell growth is a necessary condition for these circuits to show the bistability and whether bistable behavior can also be observed in conditions where the growth rate is rather dynamic.

We systematically tested the dynamic behaviors of the self-activation switch and toggle switch in different conditions with or without cell growth. We found that the memory of the self-activation switch is lost due to cell growth and thus no hysteresis is found using the dilution protocol with fresh medium. However, after uncoupling the growth feedback from gene circuits using protocols by limiting the cell growth, we found that there is a large range of bistability. We further tested the toggle switch with our protocols and found that it is refractory to growth feedback. Thus, the effects of growth-mediated feedback on gene circuits depend on their network topology. While some circuits are more robust to the perturbation from growth feedback, the functions of others are easily compromised . The underlying mechanism is demonstrated with mathematical modeling and theoretic analysis by integrating the dynamics of growth into the gene circuits.

RESULTS

Theoretical analysis of the self-activation circuit reveals bistability, but experimental data shows no memory.

To determine the effects of growth feedback on the gene circuits, we first built a simple self-activation gene circuit in which the transcriptional factor AraC forms a dimer and binds to the promoter P_{BAD} in the presence of stimulus arabinose (L-ara) and activates the expression of itself and output marker GFP (Fig. 1B). We measured the dose-response curve of the prompter P_{BAD} (dots in Fig. 1A), which shows ultrasensitivity after fitting with the Hill function (black curve in Fig. 1A). Based on the fitted parameters, we developed a mathematical model for the AraC self-activation system. Through analysis, we predicted that this system is bistable under the right conditions. As shown in Fig. 1B, the system suddenly switches on at a particular threshold as the stimulus increase if the initial state is 'OFF'. While the system stays in the 'ON' state, even the stimulus is completely removed if it is initially activated with a high dose of stimulus. Thus, theoretical analysis of our mathematical model with the parameters fitting experiment data predicts that the AraC self-activation system is bistable.

To test our prediction, we measured the response of this circuit on the dose of stimulus L-ara. Bimodal distributions were observed in a broad range of arabinose concentration (Fig. 1C), with some of the cells in the high GFP state and some in the low GFP state, suggesting the system could be bistable. However, this data is not sufficient to prove the bistability of the system. To verify this, further experiments were done to test whether the system shows hysteresis. The fraction of 'ON' cells as a function of arabinose concentration was measured under two different initial conditions. First, cells were initially in the inactive state and then treated with a series of L-ara. After 17 hours, fluorescence was measured with flow cytometry and the fractions of activated cells were measured, showing a threshold established above which the system can be activated (black line, Fig. 1D); this is consistent with the prediction. Second, the activated cells pretreated with a high dose of L-ara were washed twice with fresh LB, then diluted 100 times into fresh LB with various concentrations of arabinose. After 18 hours, the fraction of activated cells shows a curve similar to the one without pretreatment (Fig. 1D, orange line), suggesting that this self-activation circuit is either bistable within a tiny parameter range or not bistable at all . Thus,

seemingly inconsistent conclusions are found from theoretical prediction and experimental verification. These data suggest that the memory of the activated cells was lost due to some additional implicit links involved in the system.

Growth-mediated feedback disguises the bistability of the self-activation circuit.

To find out the underlying reason for the memory loss, in addition to the final steady states, we studied the dynamics of the system of activated cells post-dilution into fresh medium. After diluting the stationary phase activated cells with 1:100 ratios into fresh media with various concentration of L-ara, the cell density (measured as optical density (OD) at 600 nm) and GFP fluorescence were measured at different time points. We found that the growth of the cell for all the samples decreased as the population reached carrying capacity, following the logistic model (Fig. 2A). However, the average GFP level (GFP/OD) decreased very quickly within the exponential growth phase and reached to a fully inactivated state at 3 hours after dilution (Fig. 2B), indicating the memory loss of the circuit. Although GFP started expressing again after 3 hours and reached to different steady states depending on the L-ara level (Fig. 2D), the final dose-response curve is similar to the one initially in the inactive state (Fig. S1). It is noted that the GFP level was maintained very well for the following 6 hours when the cells reached the stationary phase, although a small decrease was found at around 10 hours. To further confirm that the memory loss does not result from the factors associated with the stationary phase, the activated cells in the log phase were diluted into fresh medium. As shown in Fig. S2, the cells are activated to different levels at OD=0.3~0.7 and still show a decline of GFP after diluted into fresh medium, consistent with the results with the dilution of cell in the stationary phase into the fresh medium. Similar phenomena were also found in the LuxR self-activation circuit (Fig. S3). Thus, fast cell division indeed can dilute the synthetic gene circuits expression.

In addition, the growth rate is decreased for the cells with the circuit compared with the cells without synthetic circuits (Fig. S4), which is consistent with the previous finding that synthetic

circuits causes burdens to the cells and inhibit cell growth [7, 21, 22, 30]. All these data suggest that dilution with fresh medium inevitably brings a growth-mediated feedback loop into the synthetic gene circuits, in which expression of the gene circuit causes burdens to the cell, and thus slows down cell growth; while fast cell growth dilutes the expression of gene circuits (Fig. 2C). That is, once the activated cells were diluted into fresh medium, there was a quick increase of cell growth that significantly diluted the gene expression of the synthetic circuits, leading to the decrease of GFP and inactivation of cells.

To demonstrate how the cell growth changes the circuit behavior, we revised our mathematical model by integrating the growth-mediated feedback (see the modeling Methods for details). A simulation was done of cells activated with a high level of L-ara diluted into the fresh medium without L-ara at both populations and single-cell levels. At the populational level, a full spectrum of AraC dynamics under different levels of L-ara is shown in Fig. 2D. Initially, AraC was set at a high level but decreased very quickly to low levels due to dilution from fast cell growth, consistent with the experimental results (Fig. 2B). At the single-cell level, several cell division events were considered for a cell post-dilution and pre-stationary phase. As shown in Fig. 2E, the AraC level is initially in high level as in the activated state (green circle in Fig. 2E) and then divided into two cells during each cell division (blue arrow with blue dashed lines in Fig. 2E) and then starts accumulating (purple arrows with solid blue lines in Fig. 2E) because of the self-activation. However, the dilution due to cell growth is much faster than the accumulation, and thus AraC levels decrease very quickly to a point below the threshold (open circle in Fig. 2E) and converges to the inactive state (the black circle in Fig. 2E) even after the cell growth becomes slower in the logistic phase and stationary phase. That is, at the early phase, the growth feedback is dominant and continuously dilutes the circuit expression. This is the underlying mechanism for the memory loss of the self-activation araC circuit and the reason why no hysteresis was found using the dilution protocol with fresh media (Fig. 2F and Fig. 1D). In the case of condition with a constant growth rate, the activation threshold of the switch increases exponentially with the growth rate

(Fig. S5). Furthermore, the deactivation threshold can be changed from negative to positive (Fig. S5). This suggests that it is unlikely to activate the system in the experiment and also is easily deactivated under the condition with a fast constant growth rate. It is worthy to note that this is consistent with previous findings that growth feedback increases the nonlinearity of one non-ultrasensitive self-activation circuit and makes it bistable [22]. Taken together, these data suggest that the underlying mechanism for the memory loss of the self-activation circuit lies on the growth feedback. That is, growth-mediated feedback disguises the bistable property of the self-activation circuit.

Decoupling of growth feedback reveals the bistability of the self-activation circuit.

The above results have shown that dilution into the fresh medium can keep cells fast-growing but inevitably induces the growth feedback to synthetic gene circuits, leading to memory loss. To decouple the growth feedback from the circuits and overcome the adverse effects, we developed a new dilution protocol. Instead of dilution into the fresh medium, we diluted cells in the conditioned medium that maintains the cells in the stationary phase. The conditioned medium was collected from the samples that were produced without any induction in parallel (Fig. 3A, left panel). The growth feedback is expected to be decoupled with this protocol (Fig. 3A, right panel).

To test this protocol, the activated cells were loaded into the microfluidic platform for live-cell analysis at the single-cell level (See methods for more details). As shown in Fig. 3B-C and Video S1-2, fresh medium was constantly provided at first and thus the GFP level was extinguished quickly along with several cell divisions, confirming the memory loss of the self-activation switch due to the growth feedback (Fig. 2B). However, the GFP level did not recover under conditioned medium with a low dose of L-ara (Fig. 3B and Video S1) although it reactivated under high dose of L-ara (Fig. 3C and Video S2), which is consistent with the results in Fig. 2B. Furthermore, we measured the dynamics of the systems under the conditioned medium at the populational level. We found that the cells did not divide as the OD was maintained in the low

level (Fig. 3D) but still had a strong ability to express the genes in the circuit since the GFP levels were maintained very well during 17 hours for all L-ara concentrations. Although some decline was found at first 2 hours (Fig. 3E), that may result from one potential cell division after dilution. It is noted that the maintance of GFP is not from slow degeratation the given the unstable GFP variant (GFP-lva) with a half-time of 40min [31]. This is consistent with the finding that a surprisingly long period of constant protein production activity has been observed in the stationary phase of bacteria [19]. Finally, a very large hysteresis range from the protocol with the conditioned medium was revealed. As shown in Fig. 3F, the cells were pretreated with a high dose of inducer and then diluted into the conditioned medium with various concentration of inducer L-ara, the fraction of activated cells shows a strong stability, indicating that the system actually functions as an irreversible bistable switch, consistent with the prediction from the mathematical model (Fig. 1B). These data suggest that growth feedback can be decoupled if the cell growth rate is decelerated. To further confirm this conclusion, we diluted the activated cells into low nutrition medium M9 with either no L-ara or with a high dose of L-ara. The memory was also maintained very well in both cases of low nutrition medium (Fig. S6A), in contrast with the sample which was diluted into high nutrition medium (Fig. S6B). **Taken together**, decoupling the growth feedback with conditioned medium from the stationary phase or low-nutrient medium maintains the memory of the gene circuits and reveals the bistability of the self-activation circuit.

The toggle switch is refractory to memory loss from the growth-mediated feedback.

We have tested the effect of the growth-mediated feedback on the synthetic self-activation circuit and found that growth-mediated feedback disguised the bistable behavior of this circuit. In order to study whether the growth feedback also affects other types of gene circuits, we tested our protocol for the toggle switch. In the original work, the author used a method to dilute cells into the fresh medium frequently to maintain the cell in the log growth phase **[26]**. They indeed found the hysteresis behavior of the toggle switch. However, the effects of growth-mediated feedback on the toggle switch are not clear. Thus, we studied the dynamics of the toggle switch with two

protocols. At the population level, after dilution of activated cells into the fresh medium which couples the growth feedback with the toggle switch circuit (Fig. 4A), the GFP decreased with time to a minimum before reaching high levels at 16 hours (Fig.4B-C). However, it is worthwhile to note that the GFP expression was not completely switched off and was reactivated for all concentrations of inducer aTC, indicating that the memory of the toggle switch was not completely lost. Similarly, after dilution of activated cells into conditioned medium to decouple the growth feedback (Fig. 4D), GFP levels of the toggle switch were also maintained very well for 17 hours (Fig. 4E-F). At the single-cell level with microfluidics, the GFP level also showed a decrease with cell division in the fresh medium regardless of the concentration of inducer aTC, but the system was reactivated after switching into the conditioned medium with both high and low doses of inducer aTC (Fig. 4GH and Video S3-4). Although GFP expression showed a heterogeneity among cells in Fig. 4GH, it is noted that it did not completely switch off, which is consistent with Fig. 4C. Furthermore, the system needed more time to recover with a low dose of inducer aTC (Fig. 4G and Video S3) in contrast to the high dose (Fig. 4H and Video S4). In Fig. 4I, the overlaid hysteresis curves with conditioned medium (green curve) and the fresh medium (red curve) showed the irreversibility of the toggle switch, consistent with previous works [26, 32, 33]. Thus, the toggle switch is refractory to memory loss from the growth-mediated feedback.

To demonstration the underlying mechanism of how the differences in the topology change the response of the self-activation switch and toggle switch to growth feedback, a simulation was done to analyze the behavior of the toggle switch. First, at the population level, no difference was found in the hysteresis curves for fast growth and no growth conditions (Fig. S7), consistent with experimental results (Fig.4I). At the single-cell level, the trajectory of one cell is shown to demonstrate how the system changes with several cell divisions and then recovers back to the original state. As shown in the directed field for the toggle switch (Fig. 4J), three fixed points exist at the intersections of the nullclines, two of which are stable and the other of which is unstable. The cell is set initially at the High-LacI/Low-TetR state, and then moves toward the left-bottom

corner (blue arrows on the dashed blue lines) due to the cell division. It tries to recover back toward the right-top corner (purple arrows on the solid blue lines) after each cell division. After several rounds of competition between the accumulation of the gene circuit production and the grow-mediated dilution, the system reaches the stationary growth phase in which cells do not divide anymore. Here, the system is still in the domain where it can be easily recovered back to the original High-LacI/Low-TetR state. It is noted that the gene circuit production is accumulating more and more as the cell growth becomes slower and slower throughout the process. One of the major differences between the self-activation switch and the toggle switch is the promoter(s) of the genes involved. In the self-activation circuit, AraC as a transcriptional activator is needed for the transcriptional activation from promoter pBAD, which drives the transcription of its own gene, thus the dilution of AraC during each cell cycle affect the accumulation of the self-activation circuit significantly as the accumulation depends on the concentration of the transcriptional activator AraC directly. In contrast, TetR as a transcription repressor in the toggle switch is not needed for the transcriptional activation but transcriptional repression from promoter pTet , which drives the expression of LacI. Thus, the production rate of LacI inversely depends on the TetR concentration and does not decrease as the growth-induced dilution makes TetR fewer. Of course, the dilution of LacI makes the repression of pLac weaker, but this repression still dominates, which maintains the system in the LacI-high state instead of switching to the TetR-high state. This difference between the toggle switch and the self-activation switch is also reflected in the direction of the dilution (blue arrows with dashed line in Fig. 2E and Fig. 4J). The dilution direction is more or less parallel to the separatrix for the toggle switch (blue dashed line in Fig. 4J), while it is vertical to the separatrix for the self-activation switch (middle black dashed line in Fig. 2E). The major difference lies in the two types of an inducible promoter that was used in these two circuits. The promoter in the self-activation circuit is positively regulated by the transcriptional factor, while the promoter in the Toggle Switch is negatively regulated by the transcriptional factor. Given that the activity of the inducible promoter pBAD directly depends on the concentration of the transcription

activator AraC, the dilution of the activator significantly decreases the production rate of the gene in the self-activation switch. While the activity of the inducible promoter pTet inversely depends on the concentration of the transcription repressor tetR, the dilution of the repressor does not decrease the relative expression of the two mutual-inhibitive genes and thus leads to the robust memory (Fig. S8). That is the reason why the system has crossed the separatrix after two cell divisions for the self-activation circuit while it still has not crossed the separatrix after four cell divisions for the toggle switch. In summary, the network topology of the toggle switch makes it robust to the growth-mediated feedback.

DISCUSSION

Host-mediated interference of circuit function depends on the topologies of the synthetic gene circuit.

It is still a big challenge to build large-sized synthetic gene circuits since often times circuits do not function as expected once they are assembled. One fundamental reason is that multiple factors of circuit-host interactions, such as metabolic burden, cell growth feedback, and resource competition are often neglected when building and testing gene circuits by assuming that these circuits are orthogonal to the host background. However, these physiological links from the host to the gene circuits create a hidden regulatory layer for synthetic gene circuits, which often perturbs the expected functions of gene circuits. In addition, it is difficult to predict how these hidden interactions affect the circuit function and how to minimize the unfavorable effects. Our data suggest that the circuit-host interaction mediated by growth feedback may disguise the true behavior of the synthetic gene circuits. Most importantly, the interference depends on the network topology of the gene circuit. While the self-activation circuit is very sensitive to the growth feedback and loses memory easily, the toggle switch is robust to the growth feedback and can maintain the circuit memory very well even though some decline was found due to cell growth. To decouple the growth feedback from the gene circuits, we tested protocols with the conditioned

medium that maintains the cells in the stationary phase or low-nutrient medium that stops the cell growth. We found that the effects of the growth-mediated feedback are minimized, and that the true behavior of the gene circuit was finally exhibited. This is consistent with the finding of different dependences on simple negative and positive regulation on growth rate [21]. The expression of one gene increases with increase of growth rate for a negative regulation, but decreases for a positive regulation [21]. Given that most synthetic gene circuits are composed of simple negative and positive regulations, the circuit-host interactions affect each link differently and thus can significantly change the functions of the gene circuits. Furthermore, it will be interesting to study how the growth-related changes in global gene expression noise affect the behavior of the circuits given the noise level is coupled with the growth rate [34]. The analysis of input-associated Signed Activation Time (iSAT) can be used in the design of robust switches that maintain a reliable memory [35, 36].

Circuit-host mutual interactions hold a double-edged effect on the gene circuits.

Here, we found that growth feedback has an adverse effect on the functions of some gene circuits as the memory can be lost due to fast cell growth. Previously, it is also found that the growth feedback lends some new properties to some gene circuits. A constitutively expressed antibiotic resistance gene shows innate growth bistability given that the expression of the resistance gene is growth-dependent and the cell growth is modulated by translation-targeting antibiotics [24]. Increased cell growth increases the expression of the resistance gene, which in turn reduces the antibiotic concentration in the cell and further promotes the cell growth. It is also found that growth feedback makes some other circuit feedback more cooperative [21, 22]. A non-cooperative circuit, autoregulation of T7 RNA polymerase, was found to generate bistability unexpectedly [22]. The underlying mechanism is that the nonlinear dilution of T7 RNA polymerase induced by growth feedback enhances overall effective cooperativity. Our results are consistent with this work: an increase in growth rate indeed increases the bistable range. However, both the activation and deactivation threshold increase with the growth rate, making the activation of the switch more

difficult and deactivation of the switch easier. Toxin cooperativity can also be induced in the multiple toxin-antitoxin systems with several growth-mediated feedbacks [25]. Thus, the effect of interactions between the circuit and the host is double-edged. While they endow new properties to some gene circuits, they impair or disguise the desired behaviors of others. Controlling strategies should be developed for the latter case. Here, we developed a strategy by controlling the growth rate to minimize the effect of the growth feedback on the memory circuits. Instead of diluting the circuits into fresh medium, conditioned medium from the stationary phase or fresh medium with minimal nutrient can be used to slow down the growth rate and thus maintain the memory of the circuits.

Conditioned medium from the stationary phase maintains the memory of the gene circuits.

Conventionally, to test the functions of gene circuits, cells are often diluted into fresh medium periodically to keep them in the log growth phase. One of the underlying reasons is that the growth rate can be maintained at an almost constant value [7, 21]. Another reason is that the primary metabolites are produced in the greatest quantities, which is important for the application of the synthetic gene circuits in industrial processes. While this dilution protocol worked successfully to demonstrate the properties of many circuits, it may cause some unexpected problems since the memory of the circuit can be lost, as shown here in this work. As for the stationary phase of bacterial, a surprisingly long period of constant protein production activity was observed [37]. This is also confirmed in our work. The expression of the circuits can be maintained in the conditioned medium for at least 17 hours. Our results suggest that the stationary phase is good to test our synthetic gene circuit. Thus, testing the gene circuit is feasible in the stationary phase, especially in the case where the growth is undesired. Given that wild bacterial in nature stay in the stationary phase most of their lifetime [37], it is very interesting to test our synthetic circuits in this overlooked physiological state and to evaluate their functions when the growth-mediated feedback is decoupled. Of course, the components in the conditioned medium are very complicated and may cause other problems. Future works are needed to further evaluate and optimize this protocol.

Bimodal distribution does not guarantee bistability.

A bimodal distribution of gene expression with distinct 'ON' or 'OFF' subpopulation is usually taken as evidence of bistability of the system. However, there are several potential sources of bimodal distribution, including positive feedback loops in synthetic gene circuits [26, 28], ultrasensitivity and stochasticity [38, 39], interplay between protein noise expression and network topologies[39], the different growth rates of subpopulations [25, 40, 41], and the feedback between cell growth and gene circuits [22, 24]. To distinguish whether the designed circuit shows ultrasensitivity or bistability, hysteresis experiments are necessary to determine if the system can maintain memory by reducing the concentration of the inducer. It is noted that all the contribution of these sources to bistability can be additive or counteractive. Thus, it is interesting to design quantitative experiments to uncouple cell growth and quantify the contribution of each source to the generation of bistability. Here, the growth feedback is decoupled by controlling the cells in the non-growth conditions and the contribution of the gene circuits to the bistability can be revealed.

Resource relocation for the synthetic gene circuits complicates the circuit-host interactions.

We demonstrated how the growth feedback affects the memory maintenances of two memory gene circuits and the underlying mechanism for why the self-activation switch is very sensitive while the toggle switch is more robust to the growth feedback. The major factor is the perturbated concentration of transcription activators and repressors due to cell growth. The activities of synthetic genes might be changed during cell division in addition to the concentration dilution due to the cell division. However, the details of how the molecular mechanism of gene activity changes during the fast cell growth phase remains unclear. One potential mechanism lies in the resource relocation strategy during cell division as extragenous synthetic gene circuits have a lower priority to be expressed than the endogenous genes. That is, the recourses such as ATP, transcriptional and translational machinery components, are biased to cell-cell-driven changes [42]. The resulting

uncertainty should be controlled as well. One strategy is to integrate the synthetic gene circuits in the cell genome [43]. Another method is to manipulate the size of the resource pools [44, 45]. Orthogonal ribosome pools or orthogonal DNA replication systems have been used to alleviate the effect of resource competition and gene coupling [46-48].

Material and Methods

Strains, media and chemicals

E. coli DH10B (Invitrogen, USA) was used for all the cloning construction experiments. Measurement of the self-activated circuit was performed in E. coli K-12 MG1655ΔlacIΔaraCBAD as described in [29]. Measurement of the Toggle switch was performed with E. coli K-12 MG1655ΔlacI as described in [32]. Cells were grown in 5ml or 15ml tubes with 220 rotations per minutes at 37 °C in Luria-Bertani broth (LB broth) with 100μg/ml chloramphenicol or 50 μg/ml kanamycin. L-Arabinose (L-ara, Sigma-Aldrich) and anhydrotetracycline (aTC, Sigma-Aldrich) were dissolved in ddH2O and later diluted to appropriate working solution.

Plasmids construction

The araC self-activation circuit was constructed into either a pSB1C3 (high copy number, used for flow cytometry and plate reader analysis) or pSB3K3 (medium copy number, used for microfluidics) backbone according to the standard molecular cloning protocols using the standardized BioBricks parts from the iGEM Registry (www.parts.igem.org). The luxR self-activation circuit was constructed into pSB1C3 backbone. The Ara C gene was amplified by PCR using the BioBrick part BBa_C0080 as the template to have the lva-tag removed. The primers used were forward 5'-ctggaattcgcggccgcttctagatggctgaagcgcaaaatgatc-3' and reverse 5'-ggactgcagcggccgctactagtagtttattatgacaacttgacggctacatc-3'. The BioBricks used were BBa_B0034 (ribosome binding site, RBS), BBa_K206000 (pBAD), BBa_K145015 (GFP with lva-tag), BBA_B0015 (transcriptional terminator) and BBa_C0062 (luxR). pLux was amplified by PCR using the BioBrick part BBa_R0062 as template. The primers used were forward 5'-

gcttctagagacctgtaggatcgtacagggttacgcaagaaaatggtttgttatag-3' and reverse 5'-ggactgcagcggccgctactagtatttattcgactataacaaaccattttc-3'. The sequence of pLux is 5'-acctgtaggatcgtacagggttacgcaagaaaatggtttgttatagtcgaataaa-3'. Detailed characterization of pLux can be found on website http://parts.igem.org/Part:BBa_R0062. All parts were firstly restriction digested accordingly using combinations of FastDigest restriction enzyme EcoRI, XbaI, SpeI and PstI (Thermo Fisher) and separated by gel electrophoresis, and then purified using GelElute Gel Extraction Kit (Sigma-Aldrich) followed by ligation using T4 DNA ligase (New England BioLabs). Then the ligation products were transformed into E. coli strain DH10B and later the positive colonies were screened. Finally, the plasmids were extracted using GenElute Plasmids Miniprep Kit (Sigma-Aldrich) and verified by sequencing. The operons constituting the self-activation circuits were constructed monocistronically. The plasmid of Toggle switch was kindly provided by Dr. James Collins as described in ref.[33] .

Hysteresis experiment

Hysteresis experiment using conditioned medium: cells were grown at 37°C on a shaker in 4ml LB broth using 15ml culture tubes. For the induction of self-activation, 2.5E-3% L-arabinose (L-ara) were added to the growth medium at the beginning of the experiment. An identical culture without arabinose was grown in parallel. When the cells had reached stationary phase, the cultures were centrifuged (2000g*5min) and supernatant from parallel culture without L-ara was sterile-filtered and used as conditioned medium. For flow cytometry and plate reader analysis, the pellet from L-ara containing culture was firstly resuspended with same volume of conditioned medium as the volume of L-ara containing medium before the centrifuge, then the resuspended cells were diluted 100 folds into culture tubes containing 1ml conditioned medium with different concentrations of L-ara added. Finally, the cells were incubated in the shaker and measured at indicated time points for flow cytometry, or loaded onto 96-well plate for plate reader analysis.

Hysteresis experiment using conditioned medium for the toggle switch was performed the same way with the induction switched to aTC.

Hysteresis experiment using fresh medium: cells were grown at 37°C on a shaker in 4ml LB broth using 15ml culture tubes. For the induction of self-activation, 2.5E-3% L-arabinose (L-ara) were added to the growth medium at the beginning of the experiment. When the cells had reached stationary phase, the cultures were centrifuged (2000g*5min) and the pellet was firstly resuspended with same volume of fresh medium without L-ara as the volume of L-ara containing medium before the centrifuge, then the resuspended cells were diluted 100 folds into culture tubes containing 1ml fresh medium with different concentrations of L-ara added. Finally, the cells were incubated in the shaker and measured at indicated time points for flow cytometry, or loaded onto 96-well plate for plate reader analysis. Hysteresis experiment using fresh medium for the toggle switch was performed the same way with the induction switched to aTC.

Flow cytometry

All samples were analyzed using Accuri C6 flow cytometer (Becton Dickinson) with excitation/emission filters 480nm/530nm (FL1-A) for GFP detection at indicated time points. 10,000 events were recorded for each sample. At least three replicate tests were performed for each experiment. Data files were analyzed with MATLAB (MathWorks).

Dynamic analysis performed by Plate Reader

Synergy H1 Hybrid Reader from BioTek was used to perform the dynamic analysis. 200 μl of culture was loaded into each well of the 96-well plate. LB broth without cells was used as a blank. The plate was incubated at 37°C with orbital shaking at the frequency of 807cpm (circles per minute). OD (optical density) of the culture was measured by absorbance at 600nm; GFP was

detected by excitation/emission at 485nm/515nm. All the measurements were taken at 30 minutes intervals.

Microfluidics and microscopy

Cells carrying the circuit of self-activation or the toggle switch were grown in 5ml LB plus indicated induction and antibiotics overnight, then the cells were centrifuged at 2000g*5min followed by resuspension into 0.5 ml fresh medium with 0.75% Tween-80 (Sigma-Aldrich) and loaded onto the device. After the cells were loaded onto the device properly, fresh media with indicated induction was supplied to the cell for 16 hours, then the cells were switched to conditioned medium with indicated induction for various amount of time as needed. Media switching was accomplished by adjusting the relative height of syringes containing fresh or conditioned medium. For details regarding design of the chip and setup of the device please refer to Hasty Lab (Microfluidics for synthetic biology: from design to execution. Methods in Enzymology). Phase and green fluorescent images were taken every 15 min under the magnification of 40X with Nikon Eclipse Ti inverted microscope (Nikon, Japan) equipped with an LED-based Lumencor SOLA SE. Perfect focus was obtained automatically using Nikon Elements software.

Mathematical modeling

<u>Self-activation Switch.</u>

In the case of **dynamic growth rate** that covers all cell growth phases from log phase to stationary phase and can be achieved by diluting cells into fresh medium, the following mathematical model was used for the self-activation switch circuit when coupled with cell growth.

$$\frac{d[araC]}{dt} = f([araC]) - d \cdot [araC] - \frac{dN}{dt}\frac{1}{N} \cdot [araC]$$

$$\frac{dN}{dt} = k_{growth} \cdot g([araC]) \cdot \left(1 - \frac{N}{N_0}\right) \cdot N$$

where $f = k_0 + k_1 \frac{Sa*[araC]^2}{Sa*[araC]^2+1}$, $Sa = C_{min} + (C_{max} - C_{min}) * \frac{Lara^n}{Lara^n+K^n}$, $g = \frac{1}{[araC]/J+1}$, [AraC] is the concentration of AraC, which is co-expressed with GFP and thus was used interchangeably. The definition and values of parameters can be found in Table S1.

When the system reaches the steady state, cells stop the growth and thus there is no changes on cell number ($\frac{dN}{dt} = 0$), and thus the third term in ODE of AraC is 0 and AraC steady state level is controlled only by the production and degradation rate, same as the case without growth feedback.

In the **case of constant growth rate** that covers only the log growth phase and can be achieved with frequent dilutions to control OD 0.3~0.4, the ODE is simplified as following

$$\frac{d[AraC]}{dt} = f(AraC) - (d + k'_{growth}) \cdot [AraC]$$

$$\frac{dN}{dt} = k_{growth} \cdot g(AraC) \cdot N = k'_{growth} \cdot N$$

The steady-state level of AraC is lower than the case of dynamic growth rate as k'_{growth} is a nonzero constant here. With increase of the growth rate constant, the steady state level of AraC can be too low to trigger the positive feedback and thus lead to an exponential increase of the activation threshold (Fig. S5).

<u>Toggle Switch.</u>

The following mathematical model was used for the toggle switch circuit when coupled with cell growth.

$$\frac{d[LacI]}{dt} = f1([LacI],[TetR]) - d \cdot [LacI] - \frac{dN}{dt}\frac{1}{N} \cdot [LacI]$$

$$\frac{d[TetR]}{dt} = f2([LacI],[TetR]) - d \cdot [TetR] - \frac{dN}{dt}\frac{1}{N} \cdot [LacI]$$

$$\frac{dN}{dt} = k_{growth} \cdot g([LacI] + [TetR]) \cdot \left(1 - \frac{N}{N_0}\right) \cdot N$$

where $f1 = crl + \frac{1.0}{1.0+\left[\left(\frac{[TetR]}{kt}\right)\cdot\left(1.0+\frac{ATc}{k_{atc}}*\frac{kt}{[TetR]}\right)^{-m}\right]^{nt}}(cil - crl)$, $f2 = crt + \frac{1.0}{1.0+\left(\frac{[LacI]}{kl}\right)^{nl}}(cit - crt)$, $g = \frac{1}{([LacI]+[TetR])/J+1}$, $[LacI]$ and $[TetR]$ are the concentration of LacI and TetR, respectively. LacI is co-expressed with GFP, and thus it was used interchangeably. The ODEs were used for the toggle switch based on our previous works [32, 33]. The definition and values of parameters can be found in Table S2.

<u>Modeling cell division events at the single-cell level.</u>

In Fig. 2E and Fig. 4J, the trajectories of the single-cell were simulated by considering several cell divisions before the system reaches the stationary phase. At each cell division, the concentrations of the variables in the synthetic circuits were set to 0.5~0.7 fold of the original values. The effects of the cell size on the concentration of variables are not considered in the model. Four cell divisions at 0.7h, 1.4h, 2.1h 3.15h were used as one example for demonstration in both the self-activation switch and the toggle switch circuits. It is noted that cell divisions are not synchronized due to the cell heterogeneities and decreased probabilities of cell division during the process, but the choice of these time points for the cell division will not affect the conclusion.

Author Contributions

X-J.T. conceived the study. X-J.T., R.Z., J.L., Q.Z. and X.W. designed the study. R.Z., J.L., P.S. and X.C. performed experiments. J.M., H.G and X-J.T. performed model studies. R.Z., X-J.T., and X.W. analyzed the data and wrote the manuscript with inputs from all authors.

Acknowledgments:

We thank X FU, J Xing, and T Hwa for valuable comments. This project was supported by the ASU School of Biological and Health Systems Engineering (to X-J.T.), NSF grant (EF-1921412) (to X-J.T.) and NIH grant (GM106081) (to X.W.). H Goetz and J Melendez-Alvarez were also supported by the Arizona State University Dean's Fellowship.

Conflict of Interest

The authors declare no competing financial interests.

Reference:

1. Brophy, J.A. and C.A. Voigt, *Principles of genetic circuit design.* Nat Methods, 2014. **11**(5): p. 508-20.
2. Liao, C., A.E. Blanchard, and T. Lu, *An integrative circuit-host modelling framework for predicting synthetic gene network behaviours.* Nat Microbiol, 2017. **2**(12): p. 1658-1666.
3. Boo, A., T. Ellis, and G.-B. Stan, *Host-aware synthetic biology.* Current Opinion in Systems Biology, 2019. **14**: p. 66-72.
4. Lynch, M. and G.K. Marinov, *The bioenergetic costs of a gene.* Proceedings of the National Academy of Sciences, 2015. **112**(51): p. 15690-15695.
5. Ceroni, F., et al., *Burden-driven feedback control of gene expression.* Nat Methods, 2018. **15**(5): p. 387-393.
6. Klumpp, S. and T. Hwa, *Growth-rate-dependent partitioning of RNA polymerases in bacteria.* Proceedings of the National Academy of Sciences, 2008. **105**(51): p. 20245-20250.
7. Scott, M., et al., *Interdependence of cell growth and gene expression: origins and consequences.* Science, 2010. **330**(6007): p. 1099-102.
8. Scott, M. and T. Hwa, *Bacterial growth laws and their applications.* Current Opinion in Biotechnology, 2011. **22**(4): p. 559-565.
9. Weisse, A.Y., et al., *Mechanistic links between cellular trade-offs, gene expression, and growth.* Proc Natl Acad Sci U S A, 2015. **112**(9): p. E1038-47.
10. Qian, Y., et al., *Resource Competition Shapes the Response of Genetic Circuits.* ACS Synth Biol, 2017. **6**(7): p. 1263-1272.

11. Erickson, D.W., et al., *A global resource allocation strategy governs growth transition kinetics of Escherichia coli.* Nature, 2017. **551**(7678): p. 119-123.

12. Venturelli, O.S., et al., *Programming mRNA decay to modulate synthetic circuit resource allocation.* Nature Communications, 2017. **8**: p. 15128.

13. Lu, T.K., A.S. Khalil, and J.J. Collins, *Next-generation synthetic gene networks.* Nature biotechnology, 2009. **27**(12): p. 1139-1150.

14. Purnick, P.E. and R. Weiss, *The second wave of synthetic biology: from modules to systems.* Nat Rev Mol Cell Biol, 2009. **10**(6): p. 410-22.

15. Kwok, R., *Five hard truths for synthetic biology.* Nature, 2010. **463**(7279): p. 288-90.

16. Purcell, O., et al., *Towards a whole-cell modeling approach for synthetic biology.* Chaos, 2013. **23**(2): p. 025112.

17. Cardinale, S. and A.P. Arkin, *Contextualizing context for synthetic biology--identifying causes of failure of synthetic biological systems.* Biotechnol J, 2012. **7**(7): p. 856-66.

18. Zhang, C., R. Tsoi, and L. You, *Addressing biological uncertainties in engineering gene circuits.* Integr Biol (Camb), 2016. **8**(4): p. 456-64.

19. Arkin, A.P., *A wise consistency: engineering biology for conformity, reliability, predictability.* Current Opinion in Chemical Biology, 2013. **17**(6): p. 893-901.

20. Klumpp, S. and T. Hwa, *Bacterial growth: global effects on gene expression, growth feedback and proteome partition.* Curr Opin Biotechnol, 2014. **28**: p. 96-102.

21. Klumpp, S., Z. Zhang, and T. Hwa, *Growth rate-dependent global effects on gene expression in bacteria.* Cell, 2009. **139**(7): p. 1366-75.

22. Tan, C., P. Marguet, and L. You, *Emergent bistability by a growth-modulating positive feedback circuit.* Nat Chem Biol, 2009. **5**(11): p. 842-8.

23. Nevozhay, D., et al., *Mapping the environmental fitness landscape of a synthetic gene circuit.* PLoS Comput Biol, 2012. **8**(4): p. e1002480.

24. Deris, J.B., et al., *The innate growth bistability and fitness landscapes of antibiotic-resistant bacteria.* Science, 2013. **342**(6162): p. 1237435.

25. Feng, J., et al., *Growth feedback as a basis for persister bistability.* Proc Natl Acad Sci U S A, 2014. **111**(1): p. 544-9.

26. Gardner, T.S., C.R. Cantor, and J.J. Collins, *Construction of a genetic toggle switch in Escherichia coli.* Nature, 2000. **403**(6767): p. 339-42.

27. Lou, C., et al., *Synthesizing a novel genetic sequential logic circuit: a push-on push-off switch.* Molecular systems biology, 2010. **6**: p. 350-350.

28. Isaacs, F.J., et al., *Prediction and measurement of an autoregulatory genetic module.* Proceedings of the National Academy of Sciences, 2003. **100**(13): p. 7714-7719.

29. Wu, F., et al., *Engineering of a synthetic quadrastable gene network to approach Waddington landscape and cell fate determination.* Elife, 2017. **6**: p. e23702.

30. Dong, H., L. Nilsson, and C.G. Kurland, *Gratuitous overexpression of genes in Escherichia coli leads to growth inhibition and ribosome destruction.* Journal of Bacteriology, 1995. **177**(6): p. 1497-1504.

31. Andersen, J.B., et al., *New unstable variants of green fluorescent protein for studies of transient gene expression in bacteria.* Appl Environ Microbiol, 1998. **64**(6): p. 2240-6.

32. Menn, D., et al., *Intracellular Noise Level Determines Ratio Control Strategy Confined by Speed-Accuracy Trade-off.* ACS Synth Biol, 2019. **8**(6): p. 1352-1360.

33. Wu, M., et al., *Engineering of regulated stochastic cell fate determination.* Proc Natl Acad Sci U S A, 2013. **110**(26): p. 10610-5.

34. Keren, L., et al., *Noise in gene expression is coupled to growth rate.* Genome Research, 2015. **25**(12): p. 1893-1902.

35. Chen, M., et al., *Noise attenuation in the ON and OFF states of biological switches.* ACS Synth Biol, 2013. **2**(10): p. 587-93.

36. Wang, L., J. Xin, and Q. Nie, *A critical quantity for noise attenuation in feedback systems.* PLoS Comput Biol, 2010. **6**(4): p. e1000764.

37. Gefen, O., et al., *Direct observation of single stationary-phase bacteria reveals a surprisingly long period of constant protein production activity.* Proc Natl Acad Sci U S A, 2014. **111**(1): p. 556-61.

38. Ochab-Marcinek, A. and M. Tabaka, *Bimodal gene expression in noncooperative regulatory systems.* Proceedings of the National Academy of Sciences, 2010. **107**(51): p. 22096-22101.

39. Birtwistle, M.R., et al., *Emergence of bimodal cell population responses from the interplay between analog single-cell signaling and protein expression noise.* BMC Systems Biology, 2012. **6**(1): p. 109.

40. Balaban, N.Q., et al., *Bacterial Persistence as a Phenotypic Switch.* Science, 2004. **305**(5690): p. 1622-1625.

41. Rotem, E., et al., *Regulation of phenotypic variability by a threshold-based mechanism underlies bacterial persistence.* Proc Natl Acad Sci U S A, 2010. **107**(28): p. 12541-6.

42. Slager, J. and J.W. Veening, *Hard-Wired Control of Bacterial Processes by Chromosomal Gene Location.* Trends Microbiol, 2016. **24**(10): p. 788-800.

43. Moon, T.S., et al., *Genetic programs constructed from layered logic gates in single cells.* Nature, 2012. **491**: p. 249.

44. Zhong, Z., A. Ravikumar, and C.C. Liu, *Tunable Expression Systems for Orthogonal DNA Replication.* ACS Synth Biol, 2018. **7**(12): p. 2930-2934.

45. Liu, C.C., et al., *Toward an orthogonal central dogma.* Nat Chem Biol, 2018. **14**(2): p. 103-106.

46. Arzumanyan, G.A., et al., *Mutually Orthogonal DNA Replication Systems In Vivo.* ACS Synth Biol, 2018. **7**(7): p. 1722-1729.

47. Darlington, A.P.S., et al., *Dynamic allocation of orthogonal ribosomes facilitates uncoupling of co-expressed genes.* Nat Commun, 2018. **9**(1): p. 695.

48. An, W. and J.W. Chin, *Synthesis of orthogonal transcription-translation networks.* Proc Natl Acad Sci U S A, 2009. **106**(21): p. 8477-82.

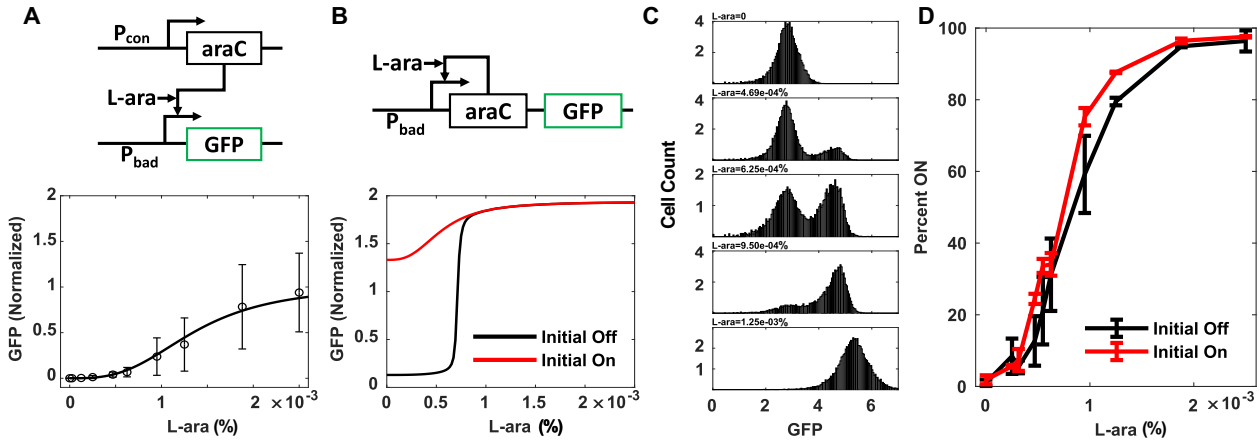

Figure 1. Theoretical analysis reveals bistability, but experimental data shows no hysteresis.

(A) Fitting the dose-response curve of the prompter (P_{BAD}) shows ultrasensitivity**.** The results showed the mean value of 6 replicates. Mean of normalized value was shown.

(B) Mathematical model predicts bistability from self-activation of P_{BAD} prompter.

(C) Bimodal distribution of the GFP shows two distinct states, 'ON' and 'OFF'.

(D) The fraction of 'ON' cell as a function of the arabinose concentration with the initial state "OFF" (blue curve) or 'ON' (Red curve) shows no hysteresis. Data displayed as mean value of three replicates.

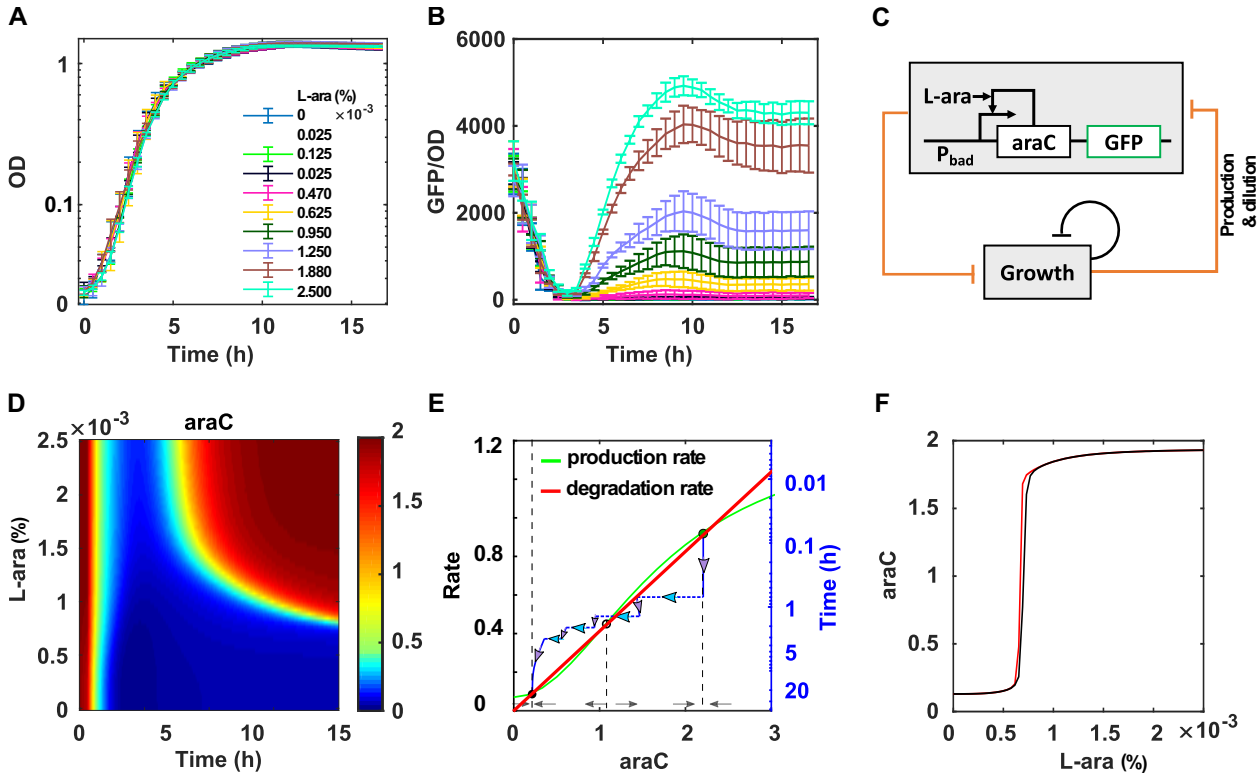

Figure 2. Growth-mediated feedback disguises the bistability of self-activation circuits.

(A-B) Dynamics of growth (OD) (A) and GFP/OD (B) after 1:100 dilution of 'ON' cells into the fresh medium with various concentrations of L-ara. Mean value of three replicates were shown.

(C) Diagram of coupling gene circuit with cell growth. The expression of gene circuit causes a burden to the cell and slow down the cell growth. Cell growth in turn dilutes or decreases the expression of the gene circuit, forming growth feedback. The mathematical model is revised based on this diagram.

(D) Simulation with revised mathematical model shows the change of AraC as a function of time and dose of inducer L-ara. The system was set to the 'ON' state initially.

(E) The process of memory loss of the self-activation switch. Simulated trajectory (blue lines) of one cell is shown on the rate balance plot of AraC. Four cell division events were considered in simulation (dashed line with arrow).

(F) Simulation confirms that the bistable range of self-activation circuit is significantly reduced with growth feedback.

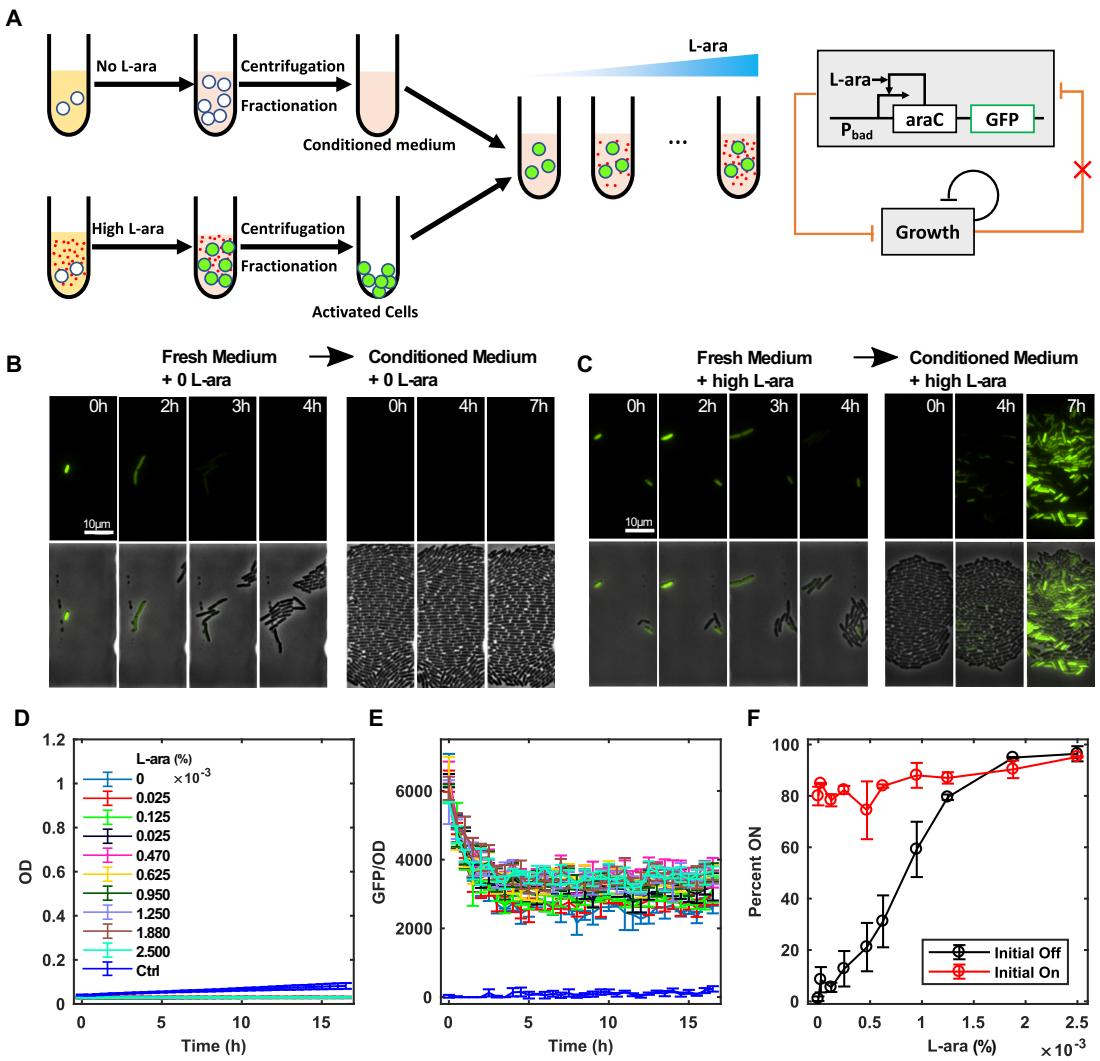

Figure 3. Decouple growth-mediated feedback reveals the bistability of the gene circuits.

(A) Diagram of the new protocol decoupling the cell growth feedback. Instead of dilution into fresh medium, cells were diluted into conditioned medium, which is from a parallel culture without any inducers in the stationary phase.

(B-C) GFP (and overlay with brightfield image) in the AraC self-activation circuit, switches off after several rounds of cell divisions with fast growth in fresh medium and then does not recover with slow/no growth in conditioned medium under a low dose of inducer (B) or recovers under a high dose of inducer (C). Representative results from three replicates are shown.

(**D-E**) The dynamics of growth (D) and GFP (E) after 1:100 dilution of activated cells into the conditioned medium with various concentration of L-ara. Negative control (blue line) was inactive cells grown in conditioned medium with no L-ara. Data indicate the mean±SD of three independent replicates.

(**F**) Hysteresis curves obtained using the new protocol by diluting 'ON' cells into the conditioned medium with various concentrations of L-ara. Mean value of three replicate tests were shown.

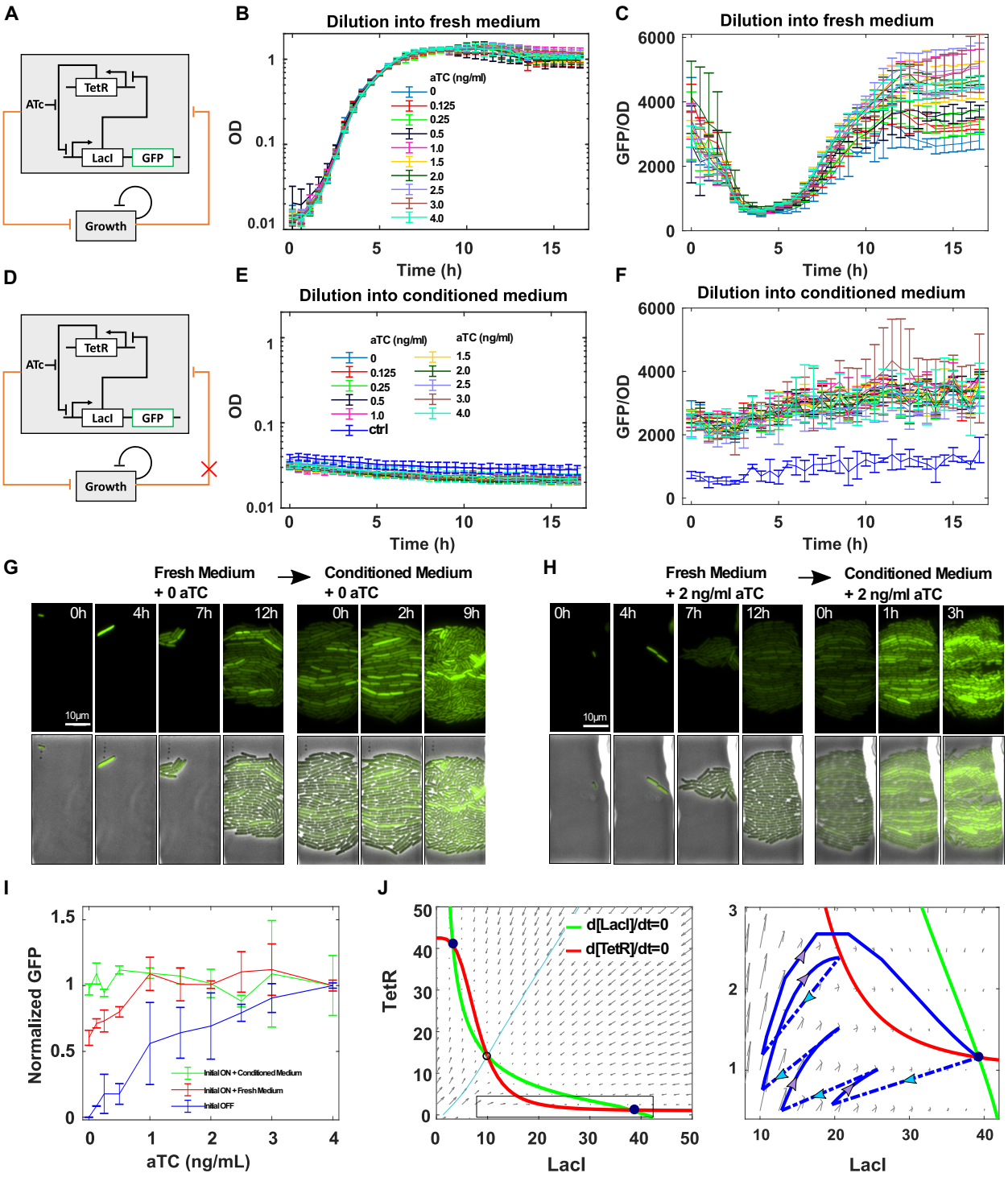

Figure 4. Toggle switch is refractory to memory loss from the growth-mediated feedback.

(A) Diagram of coupling toggle switch circuit with growth feedback in fresh medium.

(B-C) Dynamics of OD and GFP/OD after 1:100 dilution of 'ON' cells into fresh medium with various concentrations of inducer aTC. Data indicates the mean±SD of three independent replicates.

(D) Diagram of decoupling toggle switch circuit with growth feedback in condition medium.

(E-F) Dynamics of OD and GFP/OD after 1:100 dilution of 'ON' cells into the conditioned medium with various concentration of inducer aTC. Negative control (blue line) was 'OFF' state cells grown in conditioned medium with aTC. Data indicate the mean±SD of three independent replicates.

(**G-H**) Time-lapse imaging of GFP (and overlay with brightfield image) in the toggle switch circuit, switches off after several rounds of cell divisions with fast growth in fresh medium and then recovers with slow/no growth in conditioned medium under both a low dose of inducer (G) or a high dose of inducer (H). Representative results from three replicates are shown.

(I) Hysteresis curves generated by dilution of 'ON' cells either into conditioned medium (green curve) or fresh medium (red curve) with different concentrations of aTC. Three replicate tests were performed to generate each curve. Within the data set of each replicate the value of GFP corresponding to each aTC concentration was normalized to the value of GFP corresponding to the highest aTC concentration. Mean±SD of the normalized value of each curve was shown.

(J) Simulated trajectory (blue lines) of one cell is shown in the direction field of LacI/TetR. Four cell division events were considered (indicated by dashed lines with blue arrows)

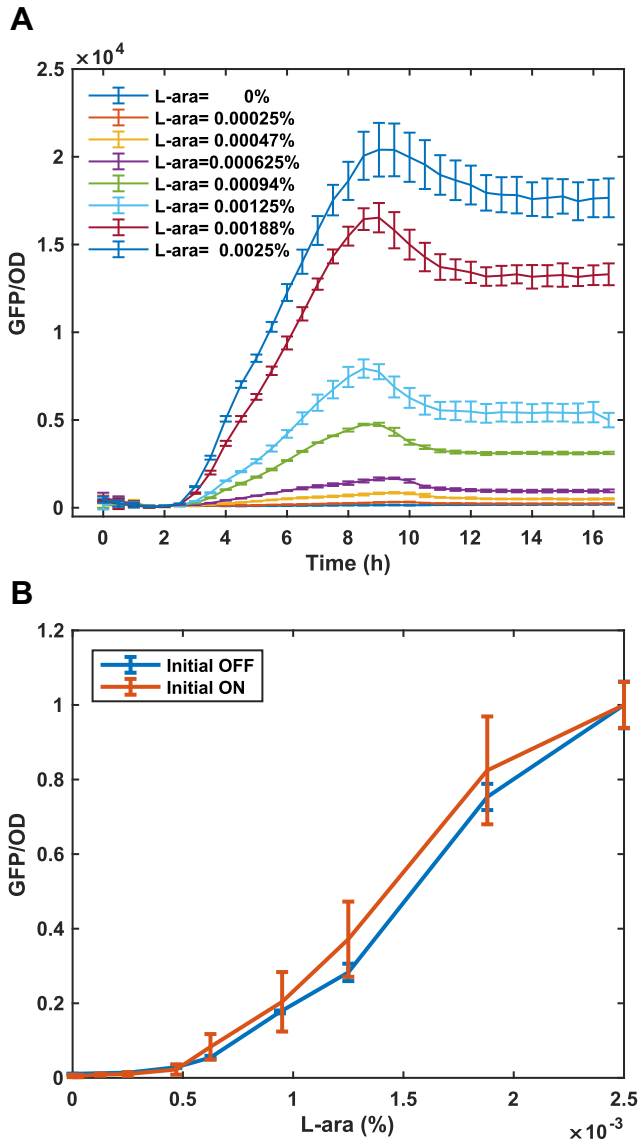

Figure S1. Similar dose-response curves with different initial states confirm the memory loss of the self-activation circuit after dilution into fresh medium. **(A)** Dynamics of GFP/OD after 1:100 dilution of 'OFF' cells into fresh medium with various concentrations of L-ara. (B) The steady-state level of GFP/OD as a function of the L-ara concentration with the initial state "ON" (red curve) is similar to the one initially in the 'OFF (blue curve). Mean value of three replicates were shown.

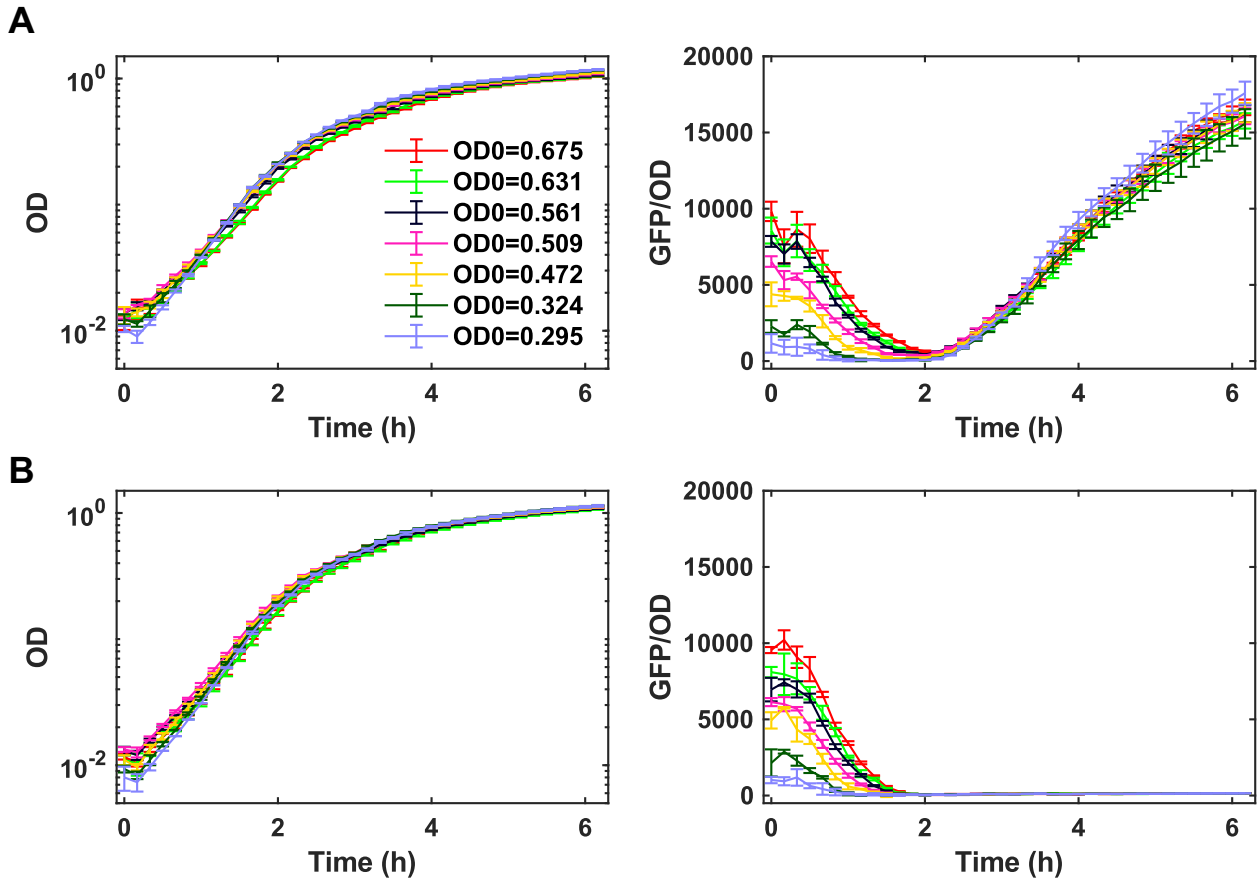

Figure S2. Memory loss of self-activation circuit was confirmed with dilution of cells in the log phase into fresh medium. The dynamics of cell growth (OD) and GFP after dilution of cell that were **activated** to different levels at OD=0.3~0.7 into fresh medium with various concentration of L-ara and high dose ($2.5*10^{-3}$%) (A) or no L-ara (B). The OD before dilution was shown as indicated.

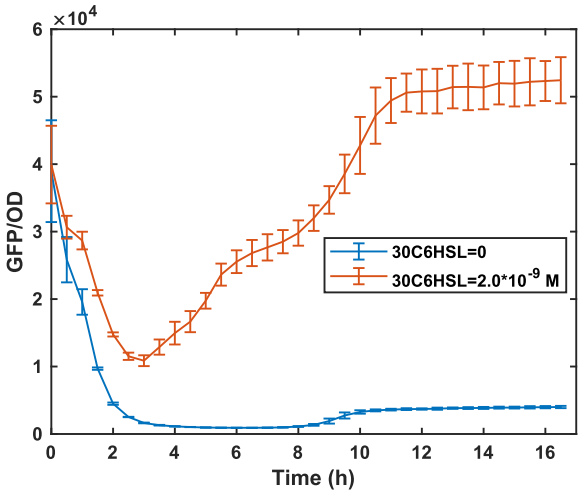

Figure S3. The dynamics of GFP after dilution of activated cells in LuxR self-activation circuit into fresh medium with high dose or no inducer 30C6HSL.

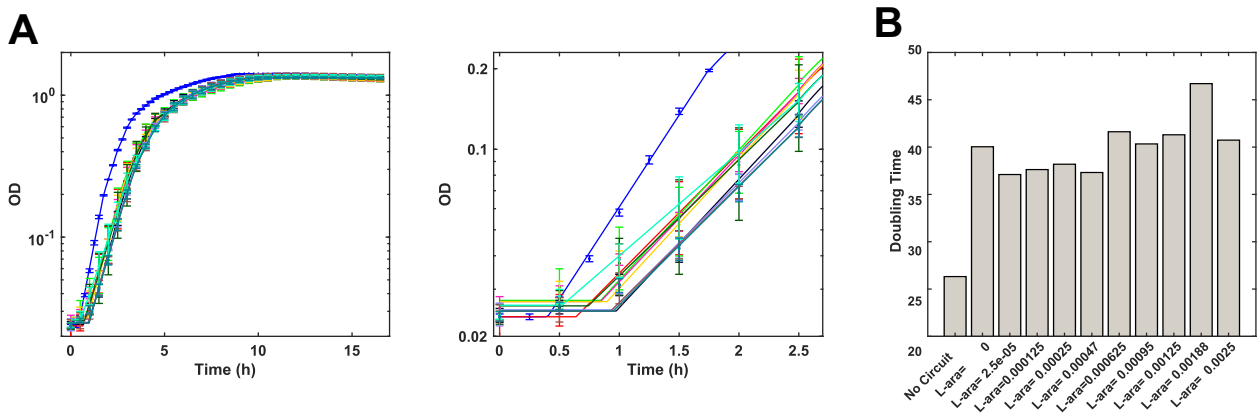

Figure S4. Inhibition of cell growth by gene circuit expression.

(A) The growth curve without or with activation of the self-activation circuit.

(B) The calculated doubling time in the exponential growth phase based on the fitting growth curve.

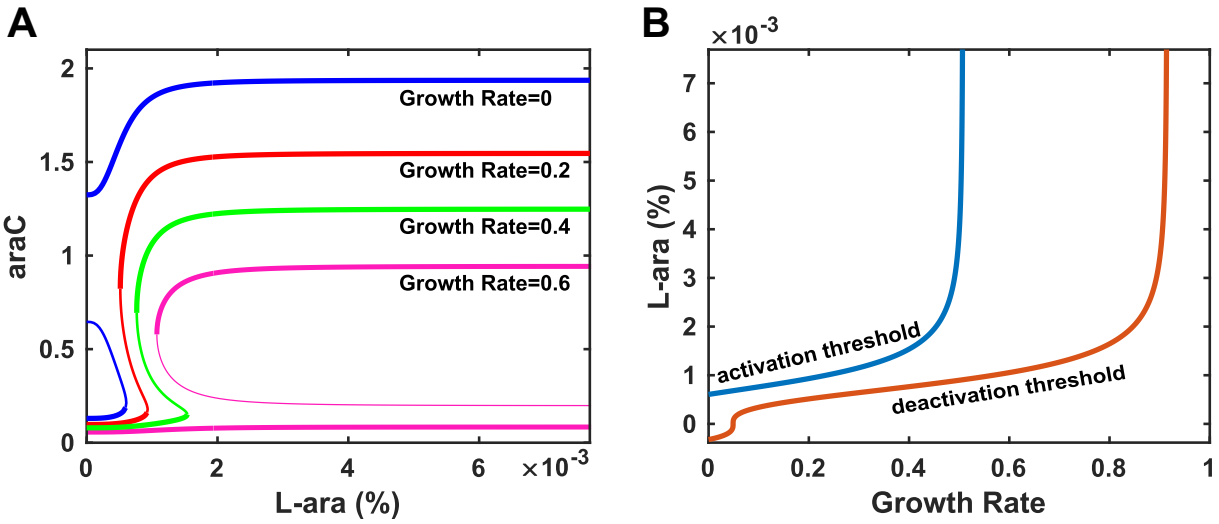

Figure S5. The effects of growth rate on the bistability of the self-activation circuit.

(A) Bifurcation diagram of AraC versus the L-ara level under conditions with various constant growth rates.

(B) Dependencies of the thresholds for activation and deactivation of the circuit on growth rate. Under the condition with constant growth rate, increasing growth rate lowers the steady-state level of AraC and increases the activation threshold of L-ara exponentially. This suggests that it is unlikely to activate the system in the experiment under a condition with a fast constant growth rate.

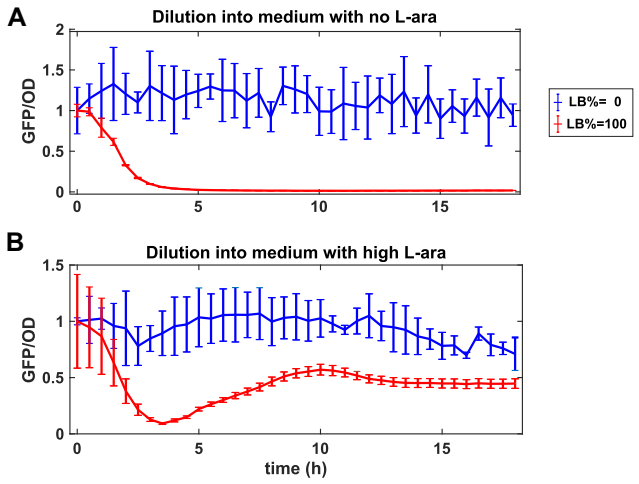

Figure S6. Decoupling of growth-mediated feedback with low-nutrient medium maintains the memory of the self-activation circuits.

The dynamics of the GFP/OD in the self-activation circuit after diluting activated cells into mediums without (A) or with high Lara (B), and low-nutrient (blue lines) or rich-nutrient (red lines).

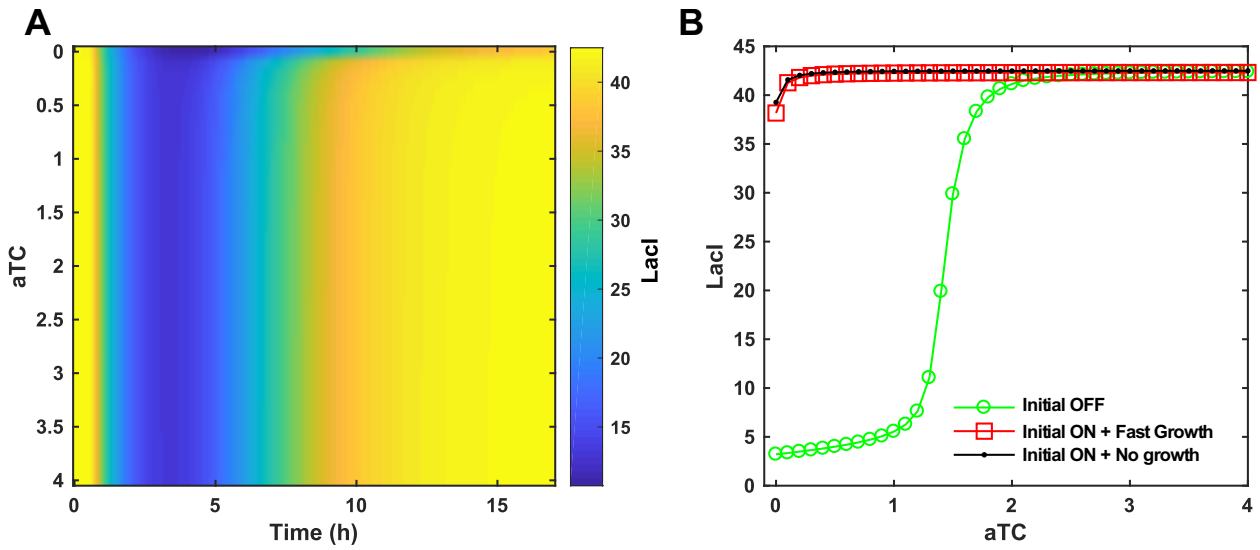

Figure S7. Simulation confirms that the memory of the toggle switch is refractory to growth feedback.

(A) Simulation with mathematical model shows the change of LacI as a function of time and dose of inducer aTC. The system was set to the activated (LacI high) state initially.

(B) The hysteresis curve for the toggle switch circuit coupled with and without growth feedback.

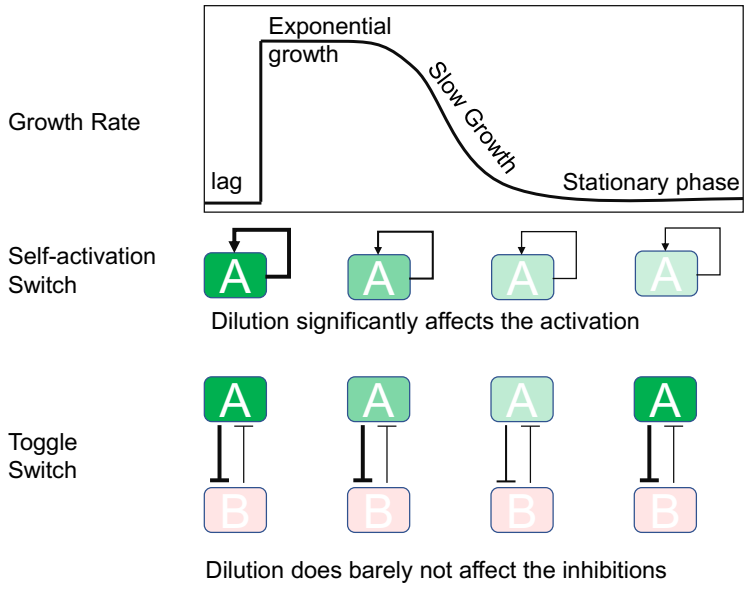

Figure S8. Schematics of how self-activation switch and toggle switch behave differently during the process of cell growth after cells dilution into fresh medium. Dilution of the gene expression significantly affects the production rate of the gene in self-activation switch and thus leads the inactivation of the switch. However, in the toggle switch, dilution of the gene expression does not affect the production rate much and relative expression levels of two mutual-inhibitive genes, and thus lead to the robust memory.

Video S1. A time-lapse movie showing the dynamics of GFP in the AraC self-activation circuit under the condition without L-ara fresh medium for 14h and conditioned medium for 7 hours thereafter. Initially the system was set in the high GFP state.

Video S2. A time-lapse movie showing the dynamics of GFP in the AraC self-activation circuit under condition with $2.5*10^{-3}$% L-ara and fresh medium condition for 14h and conditioned medium for 7 hours thereafter. Initially the system was set in the high GFP state.

Video S3. A time-lapse movie showing the dynamics of GFP in the toggle switch circuit under the condition without aTC and fresh medium for 16h and conditioned medium for 10 hours thereafter. Initially the system was set in the high GFP state.

Video S4. A time-lapse movie showing the dynamics of GFP in the toggle switch circuit under under the condition with 2ng/ml aTC and fresh medium for 16h and conditioned medium for 10 hours thereafter. Initially the system was set in the high GFP state.

Parameter	Value	Parameter	Value
$\boldsymbol{C_{min}}$	0.9	C_{max}	3
$\boldsymbol{K}$	0.5	n	3
$\boldsymbol{k_0}$	0.07	k_1	1.4
$\boldsymbol{d}$	0.7	J	1
$\boldsymbol{k_{growth}}$	2	N_0	1.35

Table S1. Fitted Parameters of the model for the AraC self-activation circuit.

Parameter	Value	Parameter	Value
$\boldsymbol{crl}$	0.5	crt	0.5
$\boldsymbol{cil}$	21.25	cit	21.25
$\boldsymbol{d}$	0.5	m	3
$\boldsymbol{nl}$	3.5	nt	1.5
$\boldsymbol{kl}$	6	kt	8
$\boldsymbol{k_{atc}}$	0.4	J	20
$\boldsymbol{k_{growth}}$	2.3	N_0	1.35

Table S2. Fitted Parameters of the model for the toggle switch circuit.